

In L. Calatroni, M. Donatelli, S. Morigi, M. Prato, M. Santavesaria (Eds.): Scale Space and Variational Methods in Computer Vision. Lecture Notes in Computer Science, Vol. 14009, Springer, Cham, 652-664, 2023.

## Image Blending with Osmosis

Paul Bungert, Pascal Peter, and  
Joachim Weickert

Mathematical Image Analysis Group, Faculty of Mathematics and Computer Science,  
Campus E1.7, Saarland University, 66041 Saarbrücken, Germany.  
{bungert, peter, weickert}@mia.uni-saarland.de

**Abstract.** Image blending is an integral part of many multi-image applications such as panorama stitching or remote image acquisition processes. In such scenarios, multiple images are connected at predefined boundaries to form a larger image. A convincing transition between these boundaries may be challenging, since each image might have been acquired under different conditions or even by different devices.

We propose the first blending approach based on osmosis filters. These drift-diffusion processes define an image evolution with a non-trivial steady state. For our blending purposes, we explore several ways to compose drift vector fields based on the derivatives of our input images. These vector fields guide the evolution such that the steady state yields a convincing blended result. Our method benefits from the well-founded theoretical results for osmosis, which include useful invariances under multiplicative changes of the colour values. Experiments on real-world data show that this yields better quality than traditional gradient domain blending, especially under challenging illumination conditions.

**Keywords:** osmosis · blending · drift-diffusion · gradient domain methods.

### 1 Introduction

Image stitching refers to the task of merging multiple images that depict different areas of the same scene or object. It has many practical applications, in particular for panorama photography [12] or various forms of remote image acquisition that create mosaic problems [4,8]. In practice, differing lighting conditions in the individual input images may yield large differences in brightness and contrast. Therefore, naïve stitching as a mosaic of the individual input images often creates undesirable boundary artefacts.

Stitching results without visible seams are the objective of so-called blending methods. Similar problems exist in image editing, which also requires seamless

merging of content from different sources. In this related field, osmosis has yielded excellent results [23,24,2]. This class of filters is inspired by physical processes. In its drift–diffusion formulation for visual computing applications, a continuous [24,19] and a discrete [23] theory have been established. Moreover, it has also been successfully used for shadow removal [24,2,15], which suggests that it performs well under large brightness differences. Despite these indications that osmosis filtering might also perform well for blending problems, its potential has not been investigated so far. Our goal is to address this problem.

### 1.1 Our Contributions

We propose an image blending approach that merges several images seamlessly by osmosis. To this end, we use derivative data of the input images to define a suitable drift vector field. It guides the osmosis process such that it converges to the blending result as a steady state.

We introduce multiple ways to construct these drift vector field and demonstrate that even straightforward approaches yield visually highly convincing results. Our evaluations on real world and synthetic data reveal that osmosis blending benefits from its multiplicative invariance, especially on challenging image sets with high contrast differences.

### 1.2 Related Work

Osmosis models in visual computing go back to Weickert et al. [24]. They have presented a continuous theory along with applications for compact image representations, shadow removal, and seamless image fusion. The continuous theory has been extended by Schmidt [19]. Vogel et al. [23] have established a discrete framework and have proposed a fast implicit solver. These considerations refer to linear osmosis models, which already allow a large degree of flexibility.

On the application side, Parisotto et al. [15] have advocated a nonlinear variant of osmosis for shadow removal. As a new application field for osmosis, Parisotto et al. [16] proposed the fusion of spectral images with linear osmosis, and they also considered nonlinear fusion approaches [14].

Osmosis models have several interesting predecessors and share some conceptual similarities with other methods. A lattice Boltzmann model for halftoning by Hagenburg et al. [9] can be seen as an early nonlinear drift–diffusion process in visual computing. Outside the field of visual computing, Hagenburg et al. [10] advocated osmosis models for improving numerical methods for hyperbolic conservation laws. They used a Markov chain formulation rather than a drift–diffusion model. In statistical physics, drift–diffusion has close ties to the Fokker-Planck equation [18] and by that connections to Langevin formulations and the Beltrami flow [21].

With its ability to “integrate” nonintegrable derivative information in a seamless way, osmosis resembles gradient domain methods. They have been introduced for shape from shading by Frankot and Chelappa [6] and have found

numerous applications in computer graphics. These include tone mapping [5] and image editing [17], but also image blending [12], as we will discuss below.

In contrast to osmosis models that are invariant under multiplicative rescalings of the pixel values, gradient domain methods are invariant under additive rescalings. Georgiev’s covariant derivative approach for image editing [7] is invariant under multiplicative changes, but has not been applied to image blending so far. Illner and Neunzert [11] have proposed directed diffusion which shares conceptual similarities with osmosis in that it converges to a so-called background image. However, they did not use it for any visual computing application.

Regarding image blending, traditional methods either attempted to find optimal boundaries between the input images in order to minimise artefacts [3] or directly average information between overlapping regions, e.g. with so-called feathering [22] or pyramid blending [1]. The gradient domain method of Levin et al. [12] not only yielded a significant gain in quality over the image domain method, but also has the closest relation to our own osmosis blending. This connection is discussed in detail in Section 2.3.

While a full review of blending is beyond the scope of this paper, there are also approaches with watershed segmentation and graph cuts [8] or wavelets [20]. Others focus on compensating colour differences [4], and there are also blending methods based on deep learning [25]. Due to its direct focus on the blending problem itself and conceptual relations, we will focus our comparative evaluation on the gradient domain method of Levin et al. [12].

### 1.3 Organisation of the Paper

In Section 2 we review the theoretical background of osmosis process which constitutes the foundation of our blending. Combining this basic model with multiple different ways to guide the osmosis-driven propagation leads to the blending approaches described in Section 3. We compare these methods against each other and gradient domain blending in Section 4 and conclude with a discussion and outlook on future work in Section 5.

## 2 Osmosis

### 2.1 Continuous Model

In our blending setting, we consider nonnegative colour images  $\mathbf{f} : \Omega \rightarrow \mathbb{R}_+^{n_c}$ . They map the image domain  $\Omega \subset \mathbb{R}^2$  to a positive colour domain  $\mathbb{R}_+^{n_c}$  with  $n_c$  colour channels ( $n_c = 3$  for RGB images,  $n_c = 1$  for greyscale). We denote individual colour channels as  $f_i$ , i.e.  $f_i : \Omega \rightarrow \mathbb{R}_+$ .

In addition to the initial image  $\mathbf{f}$ , the osmosis process also relies on a given multi-channel *drift vector field*  $\mathbf{d} : \Omega \rightarrow \mathbb{R}^{2n_c}$ . For each channel  $i$  of the image  $\mathbf{u}(\mathbf{x}, t)$ , the osmosis evolution over time  $t$  is described by the initial boundary

value problem

$$\partial_t u_i = \Delta u_i - \mathbf{div}(\mathbf{d}_i u_i) \quad \text{on } \Omega \times (0, \infty), \quad (1)$$

$$u_i(\mathbf{x}, 0) = f_i(\mathbf{x}) \quad \text{on } \Omega, \quad (2)$$

$$\mathbf{n}^\top (\nabla u_i - \mathbf{d}_i u_i) = 0 \quad \text{on } \partial\Omega \times (0, \infty). \quad (3)$$

The linear partial differential equation (PDE) (1) describes the propagation of grey levels over time  $t$ .

The evolution equation (1) consists of a diffusion part defined by the Laplace operator  $\Delta u_i = \partial_{xx} u_i + \partial_{yy} u_i$  and the drift component  $-\mathbf{div}(\mathbf{d}_i u_i) = -\partial_x d_{i,1} u_i - \partial_y d_{i,2} u_i$ . The drift vector field  $\mathbf{d}_i \in \mathbb{R}^2$  contains two-dimensional drift vectors for the colour channel  $i$ , and  $d_{i,1}$  and  $d_{i,2}$  denote its first and second components. It distinguishes osmosis from a pure diffusion process, which would lead to a flat steady state for  $t \rightarrow \infty$ . Instead, for osmosis, non-flat steady states are possible.

In addition to the image  $\mathbf{f}$  as an initial condition at time 0 in Eq. (2), we define homogeneous Neumann boundary conditions in Eq. (3). They prevent transport across the image boundaries  $\partial\Omega$  with outer normal vector  $\mathbf{n}$ .

## 2.2 Theoretical Properties

Weickert et al. [24] have shown several characteristic properties of osmosis processes. Let the average colour value  $\mu_{f_i}$  of a channel  $f_i$  be described by

$$\mu_{f_i} = \frac{1}{|\Omega|} \int_{\Omega} f_i(\mathbf{x}) d\mathbf{x}. \quad (4)$$

As for diffusion processes, this average is preserved by osmosis for all intermediate results  $\mathbf{u}(\cdot, t)$ , yielding  $\mu_{f_i} = \mu_{u_i(\cdot, t)}$ . Furthermore, all intermediate results retain their nonnegativity, i.e.  $u_i(\mathbf{x}, t) \geq 0$  for all  $\mathbf{x} \in \Omega$ ,  $i \in \{1, \dots, n_c\}$ , and  $t > 0$ .

For visual computing purposes, statements on the steady-state for  $t \rightarrow \infty$  are of particular interest. Let us first consider the so-called *compatible* case for osmosis. Here, the drift vector field  $\mathbf{d}$  fulfills

$$\mathbf{d}_i = \frac{\nabla v_i}{v_i} \quad (5)$$

for a so-called *guidance image*  $\mathbf{v} : \Omega \rightarrow \mathbb{R}_+^{n_c}$ . The corresponding drift vector field  $\mathbf{d}$  is referred to as the *canonical drift vector field* of  $\mathbf{v}$ . The steady state  $\mathbf{w}(\mathbf{x})$  of the osmosis process is given by

$$w_i(\mathbf{x}) = \frac{\mu_{f_i}}{\mu_{v_i}} v_i(\mathbf{x}) \quad (6)$$

for all channels  $i$ . Thus, the osmosis process converges to the guidance image rescaled to the average grey value of the initial image.

Note here that the definition of the canonical drift vector field in Eq. 5 implies a multiplicative invariance w.r.t. the guidance image. This is a very useful



property for visual computing applications that deal with brightness differences. Therefore, osmosis seems well-suited for blending.

In our blending scenario, we want to obtain the blended image as the steady state of an osmosis process. Since this result is unknown, we also do not have access to its canonical drift vector field. Therefore, we need to consider the so-called *incompatible case* of osmosis.

### 2.3 Incompatible Drift Vector Fields and Gradient Domain Methods

Weickert et al. [24] also consider the steady state of the osmosis evolution on the image  $\mathbf{u}(\mathbf{x}, t)$ , which implies  $\partial_t u_i = 0$  for all channels  $i$ . Plugging this into Eq. (1), the steady state result  $\mathbf{w}$  fulfills

$$\Delta w_i = \mathbf{div}(\mathbf{d}_i w_i). \quad (7)$$

This closely resembles the Poisson equation

$$\Delta w_i = \mathbf{div} \mathbf{g}_i. \quad (8)$$

It arises for so-called gradient domain methods [6,17] as a necessary condition for finding a minimiser of the energy

$$E(u_i) = \int_{\Omega} |\nabla u_i - \mathbf{g}_i|^2 d\mathbf{x}. \quad (9)$$

For a gradient field  $\mathbf{g}_i = \nabla v_i$  this yields an exact integration, and thus  $\mathbf{v}$  as a result, up to an additive constant. This corresponds to the compatible osmosis case. For our blending purposes, it will however be vital that osmosis exhibits multiplicative invariances instead.

Minimising the energy from Eq. (9) for a non-integrable vector field  $\mathbf{g}_i$  yields an approximate integration result  $\mathbf{u}_i$ . Similarly, for osmosis, we can also calculate a steady state that fulfills Eq. (7) for a drift vector field  $\mathbf{d}_i$  which does not correspond to a guidance image. This *incompatible* case allows us to design drift vector fields that can be used for blending in Section 3.

### 2.4 Discrete Osmosis

In order to apply osmosis to digital images, we use the discrete implementation proposed by Vogel et al. [23]. They have shown that the theoretical results carry over into the discrete setting and can be implemented with appropriate finite difference discretisations.

We are only interested in the steady state, i.e. the solution of the elliptic equation (7). Therefore, we use an implicit scheme with a stabilised BiCGSTAB solver as described by Meister [13], since this yields faster results compared to an explicit formulation [23].

Note that in the scheme from [23], the drift vector field is discretised on a grid shifted by  $h/2$  for a grid size  $h$ . Therefore, the discrete samples coincide with pixel boundaries. This is of particular importance for our seam removal approach in Section 3.2.

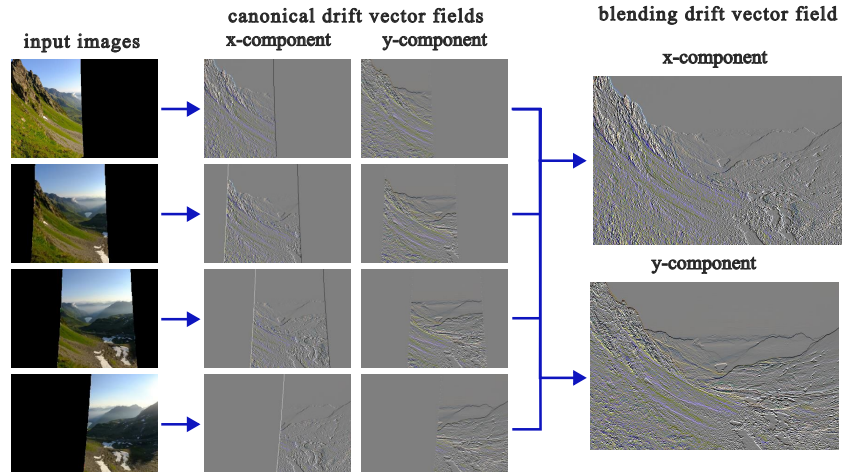


**Fig. 1. Drift Vector Blending.** The canonical drift vector fields for all input images are stitched together at the predetermined seams. The steady state of an osmosis process based on this joint blending drift vector field yields the blended image.

### 3 Blending with Osmosis

In the following we define multiple blending approaches based on the osmosis model from Eq. (1)–(3). Our blending differs only in terms of the drift vector field  $\mathbf{d}$ . For all approaches, we assume that the panoramic or mosaic images are already aligned manually or by a suitable algorithm.

All following approaches share the same basic problem formulation. Given are  $n$  aligned, partially overlapping images  $\mathbf{v}_1, \dots, \mathbf{v}_n \in \mathbb{R}_+^{n_x \times n_y \times n_c}$  with spatial resolution  $n_x \times n_y$  and  $n_c$  colour channels. Our approach merges these images into a result  $\mathbf{w} \in \mathbb{R}_+^{n_x \times n_y \times n_c}$ , the steady state of an osmosis process. As illustrated by Fig. 1, the aligned input images are padded to the target resolution  $n_x \times n_y$ .

Note that according to the properties of osmosis discussed in Section 2, the steady state is almost completely independent of the initial image. Only the average colour value in each channel carries over, otherwise the steady state is fully determined by the drift vector field. The osmosis process can thus be initialised with a naïvely stitched image or a flat image with the same average colour value. Both variants will lead to the same results. Moreover, osmosis preserves positivity, but not necessarily the maximum colour values. Therefore, we clip the osmosis steady state to the original image range  $[0, 255]$ .

#### 3.1 Drift Vector Blending

The most straightforward approach to osmosis blending is to build a composite drift vector field by stitching at a hard seam. To this end, we first compute the canonical drift vector fields  $\mathbf{d}_1, \dots, \mathbf{d}_n$  that correspond to the input images  $\mathbf{v}_1, \dots, \mathbf{v}_n$  according to Eq. (5).

We split overlapping image parts in the middle, thus partitioning the image into  $n$  parts. The corresponding drift vector fields  $\mathbf{d}_i$  form a partition of the joint drift vector field  $\mathbf{d}$  as depicted in Fig. 1. At partition boundaries, the drift vectors at the pixel boundary overlap (see Section 2.4). At such locations, we average the values of both adjacent drift vector fields.

Instead of splitting images in the middle, one can also attempt to minimise brightness differences between neighbouring pixels with an optimal seam algorithm. For our experiments we follow Levin et al. [12] and use the minimum error boundary cut [3]. It computes a seam between two image areas by minimising the overlapping error in terms of the Euclidean distance. The path along the pixel boundaries with the lowest overall error is computed with dynamic programming.

### 3.2 Seam Removal

The blending problem can be also interpreted as a generalisation of shadow removal. In both cases, there are multiple regions with different illumination and the goal is to fuse them seamlessly into a single image.

Therefore, we also investigate if established methods for osmosis-based shadow removal yield better results than the drift vector stitching. Weickert et al. [24] compute the canonical drift vector field of the image to be edited and modify it by setting the drift vector field to zero at the shadow boundaries.

After acquiring seams as in the previous section, we first stitch the images together directly in the image domain without performing any blending. This allows us to compute the canonical drift vector field of this preliminary composite image. The seams coincide with pixel boundaries, which also correspond to the locations of the drift vector field in our discretisation (see Section 2.4). Therefore, we can simply edit the drift vector field by setting it to zero at seam locations.

### 3.3 Alpha Blending with Osmosis

Levin et al. [12] also considered soft seam methods [22] for gradient domain blending. Therefore, we also investigate if this concept can be useful in the case of osmosis blending.

Soft seam approaches do not simply stitch together input data at the seams as we did in Section 3.1. Instead, they perform weighted averaging in overlapping regions. Let  $\mathbf{d}_\ell$  denote the left and  $\mathbf{d}_r$  the right canonical drift vector field in a vertically split overlapping region.

We blend the drift vector fields by location adaptive weighting, i.e. at location  $i, j$ , we get

$$\mathbf{d}_{i,j} = \alpha(i, j) \mathbf{d}_{\ell,i,j} + (1 - \alpha(i, j)) \mathbf{d}_{r,i,j}.$$

The weight  $\alpha$  changes according to its distance to the seam. For vertical seams, the shortest distance can be simplified to a description via the horizontal index

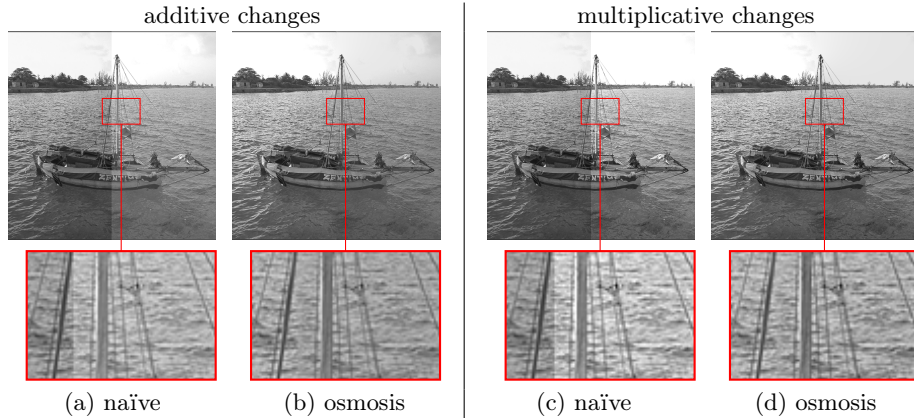


**Fig. 2. Invariance Experiments for Osmosis.** Experiments on synthetic examples show that osmosis blending removes seams convincingly for both multiplicative and additive changes.

*i.* For our experiments, we define the weight  $\alpha$  according to

$$\alpha(i, j) = \begin{cases} 1 & \text{for } i < s_j - w, \\ \frac{s_j + w - i}{2w} & \text{for } s_j - w \leq i \leq s_j + w, \\ 0 & \text{for } i > s_j + w. \end{cases} \quad (10)$$

Here,  $s_j$  denotes the horizontal position of the seam at the vertical position  $j$ . We weight both fields equally at the seam and linearly blend the two drift vector fields inside of the window  $[s_j - w, s_j + w]$  with size  $2w$ .

## 4 Experiments

All real-world images in the evaluation have been aligned and warped with the open source tool Hugin 2021.0.0<sup>1</sup>. Osmosis was implemented with an implicit scheme and a BiCGSTAB solver as proposed by Vogel et al. [23]. For each step with a time step size of  $\tau = 10^5$  this solver is stopped if the relative Euclidean norm of the residual drops below  $10^{-9}$ . We also determine the number of time steps on a relative Euclidean norm on the steady state equation (7), requiring a decay of  $\|\Delta u_i - \mathbf{div}(\mathbf{d}_i u_i)\|_2$  by more than a factor  $10^{-6}$  compared to the initialisation.

In addition to evaluating different osmosis blending variants against each other, we compare against gradient domain blending. Here, gradient fields of the input images are stitched together with the same seams as our osmosis method to allow a direct comparison between the properties of these approximate

<sup>1</sup> <https://hugin.sourceforge.io/>

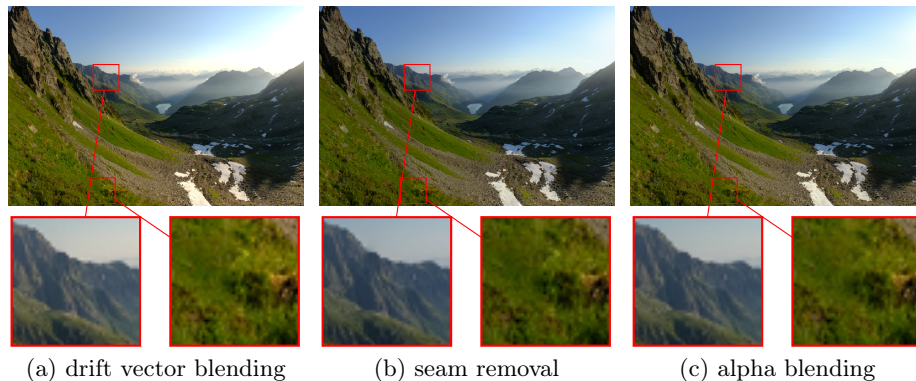


**Fig. 3. Comparison of Osmosis Blending Approaches.** The simple direct blending yields results that are just as convincing as seam removal. Alpha blending leads to blurry seams close to the camera, where alignment is imperfect.

integration methods (see Section 2.3). This corresponds to algorithm GIST2 of Levin et al. [12], a widely known approach that is conceptually closest to our own.

#### 4.1 Invariances of Osmosis Blending in Practice

In Section 2 we discussed the multiplicative invariance for the compatible osmosis case. This is the dominating type of illumination changes in blending, and we verify that this carries over to the blending application. Moreover, we also investigate the impact of additive changes and compare against naïve stitching. These are less common, but in practice, more complex mixtures of lighting changes than pure multiplicative ones can occur. Therefore we created two synthetic test cases for the image *boat* in Fig. 2. For the additive change in Fig. 2(a), each pixel value in the left image half was increased by 30, and in Fig. 2(c), each pixel was multiplied by 1.3. In both cases, the results were clipped at 255. Osmosis blending is robust under both types of brightness changes.

#### 4.2 Comparing Variants of Osmosis Blending

On the *mountain* sequence from Fig. 1 we compare our three osmosis blending approaches from Section 3. In Fig. 3, all three approaches equilibrate brightness differences well. Drift vector blending and seam removal also produce no visible artefacts at the seams. Only alpha blending leads to blur at stitching boundaries. Due to its simplicity and quality, drift vector blending is our method of choice.

#### 4.3 Plausibility Check: Low Brightness Differences

As a plausibility check, we first investigate the *mountain* sequence with visible, but fairly low brightness differences for naïve blending in Fig. 4. As expected,

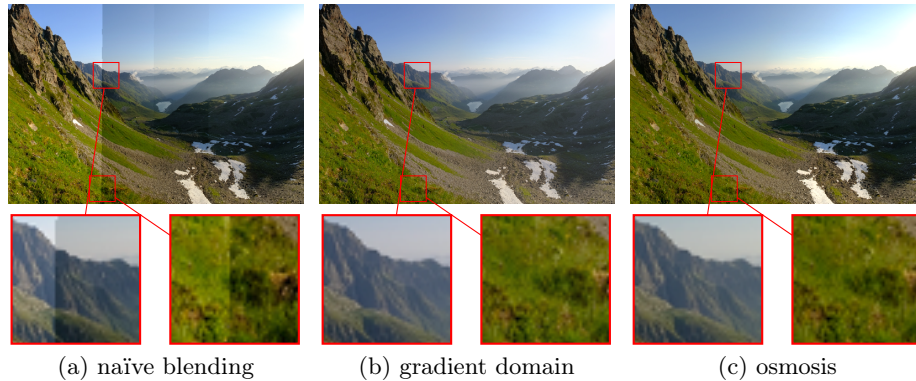


**Fig. 4. Plausibility Check: Low Brightness Differences.** As expected, on simple sequences with moderate brightness differences, osmosis and gradient domain blending both perform well. But already here, a slightly better preservance of contrast hints at the robustness of osmosis blending.

gradient domain blending yields good results without visible seams. Osmosis offers similar quality with a slightly better preservation of high contrast, such as the shadow of the mountains in the right half of the image.

#### 4.4 High Brightness Differences

We also evaluate our blending on two image sets with extreme brightness changes. These experiments reveal the differences between our osmosis blending and the gradient domain approach. For the first set, *building*, illumination changes were synthetically created in Adobe Lightroom v5.5 by darkening one half of the input images and brightening the other (by 1.5 stops). Fig. 5(a)–(c) show that with optimal seam blending, both the gradient domain approach and osmosis remove the seams. However, only osmosis is able to maintain or even enhance the contrast in the darkened image parts on the left-hand side. This highlights how the multiplicative invariance of osmosis has a significant practical impact.

The real world sequence *tracks* in Fig. 5(d)–(e) contains naturally occurring large brightness differences. Again, osmosis preserves the contrast better than gradient domain blending and yields a considerably more vivid result.

## 5 Conclusions

We have proposed the first osmosis model for image blending. Our investigation has shown that already simple stitching of drift vector fields yields excellent results without any visible seams. The natural invariances of the osmosis filter take care of multiplicative brightness differences without the need of any further processing such as alpha blending.



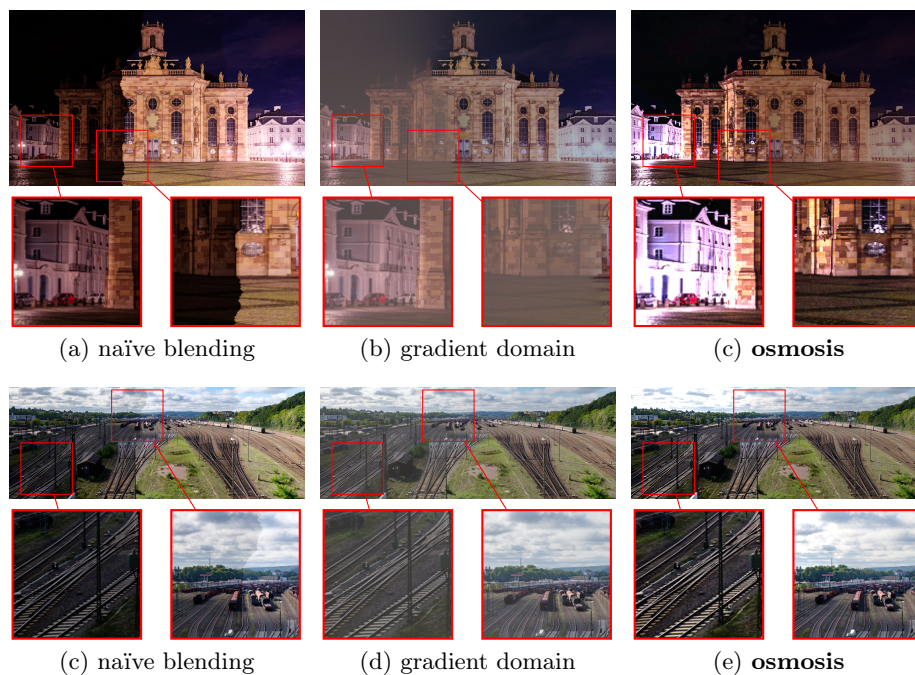


**Fig. 5. High Brightness Differences.** We perform optimal seam blending of *building* and *tracks* sequences. On these challenging sequences, osmosis preserves the image contrast significantly more convincingly due to its multiplicative invariance.

In particular for challenging image sequences with large brightness changes, osmosis clearly produces superior results compared to gradient domain methods.

This application highlights the practical value of the theoretical properties provided by osmosis filtering. In the future, we intend to leverage these strengths for additional applications in computer vision and computer graphics.

## References

1. Burt, P.J., Adelson, E.H.: A multiresolution spline with application to image mosaics. *ACM Transactions on Graphics* **2**(4), 217–236 (Oct 1983)
2. d’Autume, M., Morel, J.M., Meinhardt-Llopis, E.: A flexible solution to the osmosis equation for seamless cloning and shadow removal. In: *Proc 2018 IEEE International Conference on Image Processing*. pp. 2147–2151. Athens, Greece (Oct 2018)
3. Efros, A., Freeman, W.T.: Image quilting for texture synthesis and transfer. In: *Proc. 28th Annual Conference on Computer Graphics and Interactive Techniques*. pp. 341–346. Los Angeles, CA (Aug 2001)
4. Fang, F., Wang, T., Fang, Y., Zhang, G.: Fast color blending for seamless image stitching. *IEEE Geoscience and Remote Sensing Letters* **16**(7), 1115–1119 (Jul 2019)

5. Fattal, R., Lischinski, D., Werman, M.: Gradient domain high dynamic range compression. In: Proc. SIGGRAPH 2002. pp. 249–256. San Antonio, TX (Jul 2002)
6. Frankot, R., Chellappa, R.: A method for enforcing integrability in shape from shading algorithms. *IEEE Transactions on Pattern Analysis and Machine Intelligence* **10**(4), 439–451 (Jul 1988)
7. Georgiev, T.: Covariant derivatives and vision. In: Bischof, H., Leonardis, A., Pinz, A. (eds.) *Computer Vision – ECCV 2006, Part IV, Lecture Notes in Computer Science*, vol. 3954, pp. 56–69. Springer, Berlin (2006)
8. Gracias, N., Mahoor, M., Negahdaripour, S., Gleason, A.: Fast image blending using watersheds and graph cuts. *Image and Vision Computing* **27**(5), 597–607 (Apr 2009)
9. Hagenburg, K., Breuß, M., Vogel, O., Weickert, J., Welk, M.: A lattice Boltzmann model for rotationally invariant dithering. In: Bebis, G., Boyle, R., Parvin, B., Koracin, D., Kuno, Y., Wang, J., Pajarola, R., Lindstrom, P., Hinkenjann, A., Encarnação, M.L., Silva, C.T., Coming, D. (eds.) *Advances in Visual Computing, Lecture Notes in Computer Science*, vol. 5876, pp. 949–959. Springer, Berlin (2009)
10. Hagenburg, K., Breuß, M., Weickert, J., Vogel, O.: Novel schemes for hyperbolic PDEs using osmosis filters from visual computing. In: Bruckstein, A.M., ter Haar Romeny, B., Bronstein, A.M., Bronstein, M.M. (eds.) *Scale Space and Variational Methods in Computer Vision, Lecture Notes in Computer Science*, vol. 6667, pp. 532–543. Springer, Berlin (2012)
11. Illner, R., Neunzert, H.: Relative entropy maximization and directed diffusion equations. *Mathematical Methods in the Applied Sciences* **16**, 545–554 (1993)
12. Levin, A., Zomet, A., Peleg, S., Weiss, Y.: Seamless image stitching in the gradient domain. In: Pajdla, T., Matas, J. (eds.) *Computer Vision - ECCV 2004, Lecture Notes in Computer Science*, vol. 3024, pp. 377–389. Springer, Berlin (2004)
13. Meister, A.: *Numerik linearer Gleichungssysteme*. Vieweg, Braunschweig, 5th edn. (2015)
14. Parisotto, S., Calatroni, L., Bugeau, A., Papadakis, N., Schönlieb, C.B.: Variational osmosis for non-linear image fusion. *IEEE Transactions on Image Processing* **29**, 5507–5516 (Apr 2020)
15. Parisotto, S., Calatroni, L., Caliari, M., , Schönlieb, C.B., Weickert, J.: Anisotropic osmosis filtering for shadow removal in images. *Inverse Problems* **35**(5) (Apr 2019), Article 054001
16. Parisotto, S., Calatroni, L., Daffara, C.: Digital cultural heritage imaging via osmosis filtering. In: Mansouri, A., El Moataz, A., Nouboud, F., Mammass, D. (eds.) *Image and Signal Processing, Lecture Notes in Computer Science*, vol. 10884, pp. 407–415. Springer, Cham (2018)
17. Pérez, P., Gagnet, M., Blake, A.: Poisson image editing. *ACM Transactions on Graphics* **22**(3), 313–318 (2003)
18. Risken, H.: *The Fokker–Planck Equation*. Springer, New York (1984)
19. Schmidt, M.: *Linear Scale-Spaces in Image Processing: Drift–Diffusion and Connections to Mathematical Morphology*. Ph.D. thesis, Department of Mathematics, Saarland University, Saarbrücken, Germany (2018)
20. Sevcenco, I.S., Hampton, P.J., Agathoklis, P.: Seamless stitching of images based on a Haar wavelet 2D integration method. In: Proc. 17th International Conference on Digital Signal Processing. Kanoni, Greece (Jul 2011)
21. Sochen, N.A.: Stochastic processes in vision: From Langevin to Beltrami. In: Proc. Eighth International Conference on Computer Vision. vol. 1, pp. 288–293. IEEE Computer Society Press, Vancouver, Canada (Jul 2001)



22. Uyttendaele, M., Eden, A., Skeliski, R.: Eliminating ghosting and exposure artifacts in image mosaics. In: Proc 2001 IEEE Computer Society Conference on Computer Vision and Pattern Recognition. pp. 509–516. Kauai, HI (2001)
23. Vogel, O., Hagenburg, K., Weickert, J., Setzer, S.: A fully discrete theory for linear osmosis filtering. In: Kuijper, A., Bredies, K., Pock, T., Bischof, H. (eds.) Scale Space and Variational Methods in Computer Vision, Lecture Notes in Computer Science, vol. 7893, pp. 368–379. Springer, Berlin (2013)
24. Weickert, J., Hagenburg, K., Breuß, M., Vogel, O.: Linear osmosis models for visual computing. In: Heyden, A., Kahl, F., Olsson, C., Oskarsson, M., Tai, X.C. (eds.) Energy Minimisation Methods in Computer Vision and Pattern Recognition, Lecture Notes in Computer Science, vol. 8081, pp. 26–39. Springer, Berlin (2013)
25. Wu, H., Zheng, S., Zhang, J., Huang, K.: GP-GAN: Towards realistic high-resolution image blending. In: Proc. 27th ACM International Conference on Multimedia. pp. 2487–2495. Nice, France (Oct 2019)